Band structure and related properties of bcc niobium

A. R. Jani,* N. E. Brener, and J. Callaway
Department of Physics and Astronomy, Louisiana State University, Baton Rouge, Louisiana 70803-4001
(Received 7 July 1988)

We report self-consistent, all-electron calculations of the band structure of paramagnetic bcc niobium. Density-functional theory and the linear combination of Gaussian orbitals method were employed. Results are presented and discussed in the light of the existing theoretical and experimental data for the energy bands, density of states, Fermi surface, optical conductivity, x-ray form factors, and Compton profile. In addition, spin-polarized band-structure calculations were carried out to investigate a possible magnetically ordered state for large values of the lattice constant. A composite transition from a nonmagnetic to a low-spin ferromagnetic state and from a low to a high-spin state was found.

I. INTRODUCTION

During the last two decades the electronic band structure and allied properties of niobium have been the subject of numerous theoretical investigations.[1-23] The electronic structure of niobium is characterized by the overlap and hybridization of a rather broad *d* band with an even broader nearly-free-electron-like *sp* band. Much interest in niobium, both theoretical and experimental, has arisen due to the fact that it has the highest superconducting transition temperature ($T_c = 9.25$ K) of all the elements in the Periodic Table. This makes the comparison of theoretical and experimental results particularly interesting. There is a large amount of experimental information available[24-53] which can be interpreted with the aid of band-structure calculations. The present study is devoted to the computation of energy bands, the density of states, the Fermi surface, the optical conductivity, x-ray form factors, and the Compton profile, which are compared with experiment wherever possible.

Recently, interest has arisen in the magnetic ordering of transition metals in nonequilibrium geometries (expanded lattices or different structures) from both experimental[54-60] and theoretical[61-70] points of view. Experimentally, thin films are grown epitaxially on appropriate substrates.[54,55] This may give a different structure and lattice constant to the film in comparison to bulk material. As an example, we mention the case of fcc iron. It has been stated that films of fcc iron grown on copper surfaces may be either ferromagnetic or antiferromagnetic, depending on the crystallographic surface where the growth occurs.[56-58] More recently, it has been conclusively demonstrated that films of fcc iron are ferromagnetic if the lattice constant is large enough.[59,60] Due to such experimental results, the study of magnetic properties of materials with respect to variation of the lattice constant has become an exciting problem from the theoretical point of view as well.[61-70] In this paper we have investigated the electronic structure of niobium at expanded lattice constants, and have found transitions to a low-spin, and then to a high-spin, ferromagnetic state.

Our computational procedures are briefly described in Sec. II. The band structure and density of states under normal conditions are presented in Sec. III. Our results are compared with those of numerous previous calculations. The Fermi surface is described in Sec. IV, and the areas of some cross sections are compared with experiment. The optical conductivity is given in Sec. V, while Sec. VI contains results for the x-ray form factors and Compton profile. The calculations for expanded lattice constants leading to possible ferromagnetic states are reported in Sec. VII. Finally, our conclusions are summarized in Sec. VIII.

II. COMPUTATIONAL METHOD

Our computational procedures are summarized very briefly below.

We have used the linear combination of Gaussian orbitals (LCGO) method as contained in the BNDPKG programs.[71] The calculations are made based on the local-density approximation to the density-functional theory. This method has been successfully applied to several metals.[65-67,72-75]. It does not require any shape approximations to charge densities or potentials. Details of the method can be found in Ref. 71.

The Bloch wave functions needed in the self-consistent calculations were expanded in a set of independent Gaussian orbitals,[76] including in this case sixteen of *s* symmetry, twelve *p*, eight *d*, and one *f*. We employed the basis set for Nb given by Poirier *et al.*,[76] except that the most diffuse *s*-orbital exponent was deleted and a single *f* orbital of exponent 0.8 was added. The exchange-correlation potential is treated in the manner described in Ref. 75. Relativistic effects are not included. The Hamiltonian and overlap matrices considered in the computations are of dimension 99×99. The lattice constant *a* of niobium at 0 K was estimated to be 6.227 a.u. using the measured thermal expansion. In the calculations the iterations leading to self-consistency were continued until the change in the leading Fourier coefficient of potential became 10^{-4} Ry or less. After establishing the self-consistency, energy levels and wave functions were evaluated at 506 points in the irreducible wedge ($\frac{1}{48}$) of the

TABLE I. Selected energy separation (in mRy) of Nb band structures.

Reference	Method	$\Gamma_{25'}$-Γ_1	$H_{25'}$-Γ_1	$H_{25'}$-H_{12}	E_F-H_{12}	E_F-Γ_1	N_1'-Γ_1
present work	LCGO[a]	404	792	687	282	387	577
2	APW[b]	428	828	755	314	387	553
7	RAPW[c]	471	868	704	279	442	
10	KKR[d]	410			302	387	
11	MBP[e]	433	795	613	243	425	570
13	LMTO[f]	480			304	452	

[a]Linear combination of Gaussian orbitals.
[b]APW calculations, exchange only ($\alpha=\frac{2}{3}$).
[c]Relativistic APW calculations, exchange only ($\alpha=\frac{2}{3}$).
[d]Green's-function method.
[e]Mixed-basis pseudopotential.
[f]Linear muffin-tin orbital.

Brillouin zone. The density of states was obtained by employing the linear analytic tetrahedron method.[77–81] The procedures used in our calculations of the Compton profile[82,83] and the optical conductivity[84–86] have been described elsewhere.

III. BAND STRUCTURE AND DENSITY OF STATES

The calculated energy bands are displayed along certain symmetry directions in Fig. 1. We also give the comparison of our results in Table I with those of other self-consistent calculations for selected energy separations.

Generally, the calculated band structure is quite similar to that of vanadium except that the d band is slightly broader here. The conduction electrons fill all of the first bands, while second and third bands are partly filled. The width of the occupied portion of the d band measured by $E_F-E(N_1)$ is 0.2675 Ry and the total d-band with including unoccupied states (estimated as N_3-N_1) is 0.5512 Ry. The total occupied bandwidth, including s states below the d band $[E_F-E(\Gamma_1)]$ is 0.387 Ry. This occupied bandwidth seems to be in good agreement with the experimental value 0.37 Ry.[87,88]

In order to have a meaningful comparison of calculations, we have listed in Table I only those which are said to be self-consistent. However, there are a large number of non-self-consistent calculations which give results at least generally consistent with those shown (i.e., we did not find any general pattern to the differences between energy levels in self-consistent and non-self-consistent results). Among the self-consistent calculations, the spreads in values of the energy differences are roughly 10% of the average values. While there are differences in

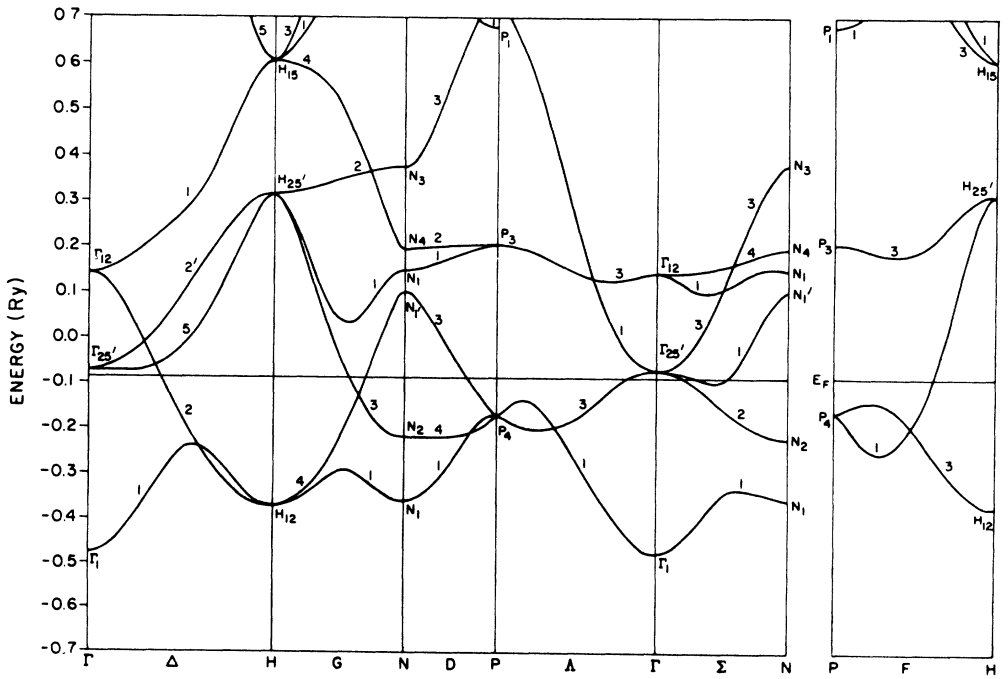

FIG. 1. Energy bands of niobium.

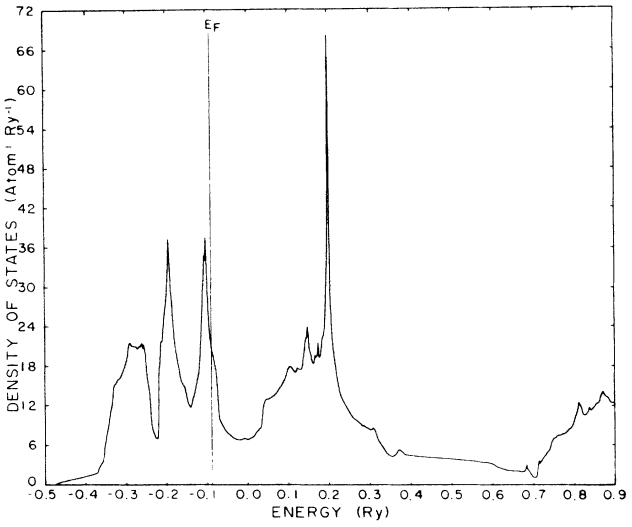

FIG. 2. Density of states of niobium.

the lattice constants used by different authors, these are much too small to account for this spread. There appear to be two major contributions to variation in energy differences: (1) use of different exchange-correlation potentials, and (2) inclusion of relativistic effects. Our present results appear to be closest to those of Ref. 10, which employs a similar but not identical expression for V_{xc}. Inclusion of relativistic terms seems to have the effect of lowering the energies of predominately s states relative to d states. Experimental information is inadequate to enable a meaningful evaluation of calculations in regard to energy differences at this time.

The density of states is shown in Fig. 2. We find a value of the density of states at the Fermi energy as $N(E_F)=20.868$ Ry^{-1}. Eastman[35] has measured photoemission from niobium and reported three peaks at 0.4, 1.1, and 2.3 eV below E_F. These peaks correlate fairly well with those in our calculated density of states. In addition to this, we have listed the density of states at the Fermi energy from different calculations in Table II. It can be seen from this table that there is a rather large spread in the values that have been found for this quantity. Most of the results are in the range 19–22 Ry^{-1}, as ours is, but there are a few well outside. No clear choice is available. Using our value of $N(E_F)$, we obtain a value 3.63 mJ mol^{-1} K^{-2} for the electronic specific-heat coefficient γ. The experimental[89] value is 7.8 mJ mol^{-1} K^{-2}. An enhancement factor of 2.15 is obtained from our results, which is higher than McMillan's value of 1.82.[23] As several anomalies in phonon dispersion curves have been reported,[90,91] it is probably that most of the enhancement is due to the electron-phonon interaction.

TABLE II. Density of states at Fermi energy in (Ry^{-1} atom^{1}).

Reference	$N(E_F)$
present work	20.868
1	19.774
2	28.200
5	22.400
6	29.930
8	21.280
10	19.050
13	21.880
17	19.860
22	19.910
23	24.800
46	18.496

IV. FERMI SURFACE

We have studied the Fermi surface of niobium constructed on the basis of our calculations. The situation for such metal in this regard is somewhat delicate as the Fermi energy falls near the energy-band state with $\Gamma_{25'}$ symmetry. After preliminary experimental investigations by several workers,[25–31] the de Haas–van Alphen study of niobium of Karim *et al.*[32] provides the most detailed information about the Fermi surface of this metal.

Principally, the second zero contains a hole surface centered at the zone center, while in the third zone there is an open surface of holes called a "jungle gym" along the ⟨100⟩ directions. The third zone also contains a set of distorted hole ellipsoids centered at N points. In addition to this, electron orbits also exist in the third zone around the closed jungle gym. The cross sections of the niobium Fermi surface obtained from our work in (100) and (110) planes are shown in Figs. 3 and 4. Points on the Fermi surface were located by interpolation.

We could estimate some cross-sectional areas from our plots in accord with a model discussed in the latest experimental report.[32] Our values are presented and compared with experimental as well as earlier theoretical values in

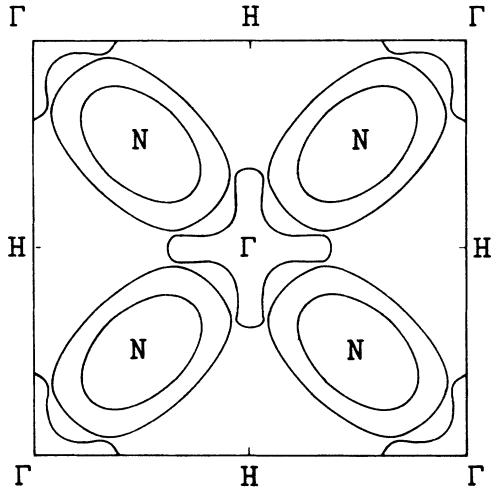

FIG. 3. Cross sections of the niobium Fermi surface in a (100) plane.

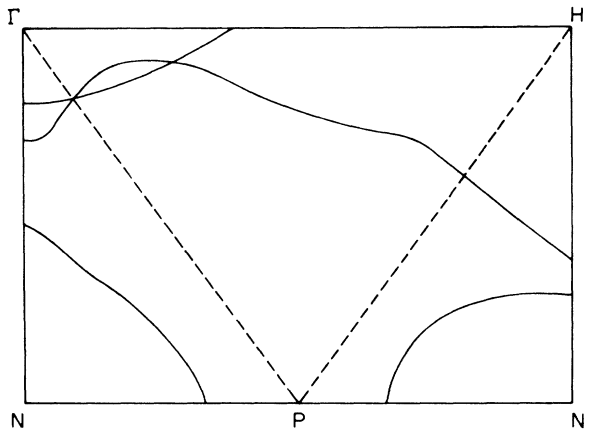

FIG. 4. Cross sections of the niobium Fermi surface in a (110) plane.

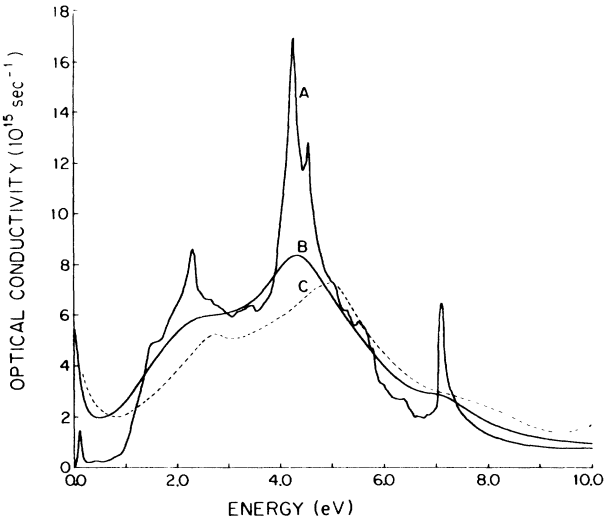

FIG. 5. Optical conductivity of niobium. Curves: *A*, interband conductivity; *B*, conductivity including lifetime broadening and a free-electron (Drude) contribution; *C*, experimental curve.

Table III. Deviating from the usual practice, we have followed the notations used in the experimental investigations.[32] It can be inferred from Table III that, except for ν_{12} and Δ orbits in the (100) plane,[12] the rest of our values are in reasonably good agreement with the experimental findings. The other features regarding the shape, such as jungle gym, distorted ellipsoids centered at *N*, an octahedron around Γ, etc., are quite similar to those reported previously.[1-3,8,9,20]

V. OPTICAL CONDUCTIVITY

The interband optical conductivity in the present work has been evaluated by performing the integration numerically in the $\frac{1}{48}$ of the Brillouin zone. The standard formula used for the computations is given in many texts.[83,92] As we could determine the momentum matrix elements analytically by using a basis set of Gaussian orbitals, the necessary **k** dependence is retained. The technique employed in the tetrahedral integration is basically that reported earlier.[71]

There have been several attempts to measure the optical conductivity of niobium in different energy ranges.[42-46] To our knowledge, no theoretical results for the optical conductivity of Nb in detail are available. Therefore, initially the interband portion of the conductivity is calculated at energies between 0.01 and 10 eV. The results are shown in Fig. 5 by curve *A*. To take into account the intraband conductivity, the contribution due to a Drude term is incorporated as described in Ref. 84. The Drude parameters $\sigma_0=3.9\times10^{15}$ sec^{-1} and $\tau'=5.51\times10^{-15}$ sec were selected from the work of Lenham and Treherne.[93] As we have done previously,[74,85] a relaxation time $\hbar/\tau=0.5$ eV was used to smooth the sharp structure of curve *A* in Fig. 5. Curve *B* in the same figures shows the optical conductivity after these corrections. The experimental curve is displayed by a dashed line (curve *C*) which has been copied from graphically presented data.[43,46] In the experimental reports[42-46] two principal maxima are observed in the (2–3) and (4–5)-eV regions. Comparison of our results with the experimental curve shows that the calculated peaks are in about the correct positions. However, we could not reproduce an observed minimum[43] around 9 eV in our theoretical plot. We note here that the situation regarding magnitude of the optical conductivity may be improved by including the self-energy correction empirically through a procedure discussed by Janak *et al.*[94] In fact, we found that the choice of the empirical renormalization factor λ (=0.07) can improve the match with the experimental curve.

On the basis of the band structure of Nb (Fig. 1), we

TABLE III. Areas (in Å^{-2}) of some cross sections of the Fermi surface of niobium.

Plane	Orbit	Present work	Expt. (Ref. 32)	Ref. 1	Ref. 2	Ref. 7	Ref. 8	Ref. 20
(100)	ν_{12}	0.728	0.6392	0.642	0.640	0.678	0.640	0.660
	ν_{3-6}	0.847	0.8145	0.855	0.820	0.884	0.820	
	α	0.114	0.1380	0.117	0.130	0.118	0.160	0.120
	β	0.101	0.0818					
	Δ	1.575	1.448	1.494		1.501	1.430	
(110)	ν_1	0.738	0.7610	0.762	0.730	0.824	0.750	0.730
	ν_2	0.924	0.8603	0.940	0.960	0.920	0.860	0.880

find that major contributions to the interband optical conductivity result from transitions along the Σ axis and near the N points. Moreover, it can be seen from Fig. 5 that in the case of Nb the onset of the transition starts very near 0 eV, which does not occur in some other metals.[74,75,92,95,96] Unfortunately, due to the Drude conductivity this feature is unlikely to be observable experimentally.

VI. X-RAY FORM FACTORS AND COMPTON PROFILE

The x-ray-scattering from factors emerging from our calculations are given in Table IV. The (1,1,0) and (2,0,0) form factors have been determined experimentally by Terasaki *et al.*[97] We also give in the same table the calculated values of atomic-scattering factors due to Hanson *et al.*[98] It is quite clear from the Table IV that our calculated values agree with the experimental ones, while the scattering factors computed from atomic Hartree-Fock-Slater wave functions[98] are slightly higher. This implies that the electronic charge distribution in bulk niobium is slightly more diffuse than that resulting from a superposition of free-atom densities. Elyashar and Koelling[7] have also obtained the x-ray form factors of Nb in their relativistic APW calculations, but they have not compared their results with experimental values. As they have only given a plot of the form factors, we could not compare explicitly our values with their graphical representation.

We have also computed the Compton profile of niobium by employing the wave functions generated in the band calculation on a mesh 506 points in the irreducible wedge of the Brillouin zone. The basic definition of Compton profile is given as[82]

$$J(q)=\frac{\Omega}{(2\pi)^3}\int d^3p\,\rho(\mathbf{p})\delta(q-\mathbf{p}\cdot\hat{\mathbf{k}})\,, \tag{6.1}$$

where $\rho(\mathbf{p})$ is the electronic momentum density and q is the magnitude of the momentum along the scattering vector. The normalization condition on the profile is given by

$$\int J(q)dq=n_e\,, \tag{6.2}$$

in which n_e is the number of electrons per atom.

TABLE IV. X-ray form factors of niobium.

Wave vector $a\mathbf{K}/2\pi$	Present calc.	Expt. (Ref. 97)	Atomic scat. factors (Ref. 98)
(1,1,0)	31.285	31.35±0.05	31.94
(2,0,0)	27.443	27.47±0.11	27.85
(2,1,1)	25.005		
(2,2,0)	23.185		
(3,1,0)	21.741		
(2,2,2)	20.682		
(3,2,1)	19.717		
(4,0,0)	18.853		
(3,3,0)	18.176		
(4,1,1)	18.152		
(3,3,0)/(4,1,1)	1.0013		
(4,2,0)	17.507		
(3,3,2)	16.925		
(4,2,2)	16.355		
(4,3,1)	15.829		
(5,1,0)	15.809		

TABLE V. Calculated Compton profile (only the band electrons are included) for niobium in the symmetry directions along with the directional average.

Q (a.u.)	$J_{[100]}$	$J_{[110]}$	$J_{[111]}$	J_{av}
0.0	1.921	2.421	2.452	2.286
0.1	2.084	2.381	2.472	2.320
0.2	2.237	2.304	2.375	2.303
0.3	2.226	2.163	2.226	2.197
0.4	2.079	2.008	1.965	2.017
0.5	1.931	1.869	1.826	1.876
0.6	1.903	1.727	1.710	1.773
0.7	1.851	1.610	1.626	1.683
0.8	1.716	1.535	1.562	1.594
0.9	1.348	1.382	1.455	1.391
1.0	0.989	1.193	1.058	1.100
1.1	0.899	1.016	0.774	0.920
1.2	0.880	0.809	0.681	0.796
1.3	0.722	0.585	0.668	0.645
1.4	0.498	0.458	0.580	0.501
1.5	0.341	0.378	0.406	0.374
1.6	0.268	0.267	0.289	0.273
1.7	0.225	0.233	0.241	0.233
1.8	0.195	0.208	0.210	0.205
1.9	0.160	0.185	0.182	0.177
2.0	0.135	0.156	0.155	0.150
2.1	0.142	0.140	0.125	0.137
2.2	0.148	0.128	0.111	0.129
2.3	0.123	0.104	0.101	0.108
2.4	0.086	0.088	0.098	0.090
2.5	0.060	0.074	0.090	0.074
2.6	0.049	0.061	0.067	0.059
2.7	0.043	0.048	0.043	0.045
2.8	0.038	0.040	0.034	0.038
2.9	0.031	0.035	0.030	0.032
3.0	0.025	0.029	0.027	0.027
3.1	0.024	0.025	0.025	0.025
3.2	0.024	0.023	0.024	0.024
3.3	0.022	0.020	0.021	0.021
3.4	0.019	0.017	0.019	0.018
3.5	0.016	0.016	0.016	0.016
3.6	0.015	0.015	0.015	0.015
3.7	0.014	0.014	0.015	0.014
3.8	0.013	0.013	0.014	0.013
3.9	0.011	0.012	0.012	0.012
4.0	0.009	0.011	0.011	0.011
4.1	0.009	0.011	0.010	0.010
4.2	0.011	0.010	0.011	0.011
4.3	0.012	0.010	0.011	0.011
4.4	0.011	0.010	0.010	0.010
4.5	0.010	0.009	0.008	0.009
4.6	0.010	0.009	0.007	0.009
4.7	0.009	0.009	0.007	0.008
4.8	0.009	0.009	0.009	0.009
4.9	0.007	0.009	0.010	0.009
5.0	0.007	0.009	0.009	0.008

The procedures used in the calculations are as described earlier.[82] Our calculations included only band electrons ($4d$,$5s$). The numerical values of the Compton profile in the three principle symmetry directions along with the angular average are listed in Table V. The directional anisotropy in the calculated Compton profiles of niobium is shown in Fig. 6. Other calculations of the Compton profile for this metal are reported by Wakoh *et al.*[38] and Papanicolau *et al.*[18] The former work is for the [100] and [110] directions, while the latter have given the results for the principal symmetry directions. We could judge that our results for the anisotropy are in good agreement with those of Wakoh *et al.*[38] We cannot compare individual values explicitly because no appropriate table of data is given in that paper. In comparing our results of Table V with Papanicolau *et al.*,[18] we saw that for small q our values are smaller than theirs and that for large q they are slightly higher. Probably this discrepancy is due to the different approaches for the generation of wave functions and we have more reciprocal-lattice vectors in the calculation, but the overall general features, like the positions of the wiggles in the anisotropic curves, are almost identical.

There have been several observations[37–40] pertaining to both the isotropic and the directional Compton profiles of niobium, but, among these, the measurements of Tomak *et al.*[40] are the most recent on polycrystalline niobium using 60-keV γ rays. We compare their results with our calculated values of the Compton profile in Fig. 7. We obtained our theoretical curve by adding, to the calculated average of the Compton profile, the necessary core contribution from Biggs *et al.*[99] In the same Fig. 7, we also give similar results due to other calculations based on a renormalized-free-atom (RFA) model.[40] It is evident from Fig. 7 that our theoretical results compare well with the experimental findings. Alexandropoulos and Reed[39] have reported the measured anisotropy of niobium for the [100] and [110] directions only. They have not corrected their data for the spectrometer-resolution function. Therefore, while making a broad comparison between our curve for [100] and [110] in Fig. 6, we found that the amplitude of our results is greater than that predicted by the experiment.[39] However, the maxima and minima in our curve occur almost near the same positions as shown in the experimental work.[39] Shiotani *et al.*[37] have also determined the anisotropy curves by measuring the angular distribution of positron-annihilation radiation in niobium. It is difficult, however, to make a quantitative comparison with their results. Therefore, we only claim that our anisotropic curves are qualitatively similar to those obtained by Shiotani *et al.*[37]

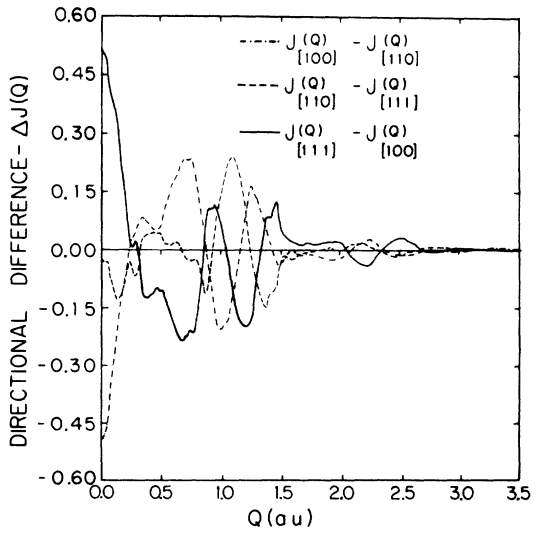

FIG. 6. Theoretical anisotropy curves of the Compton profile in niobium.

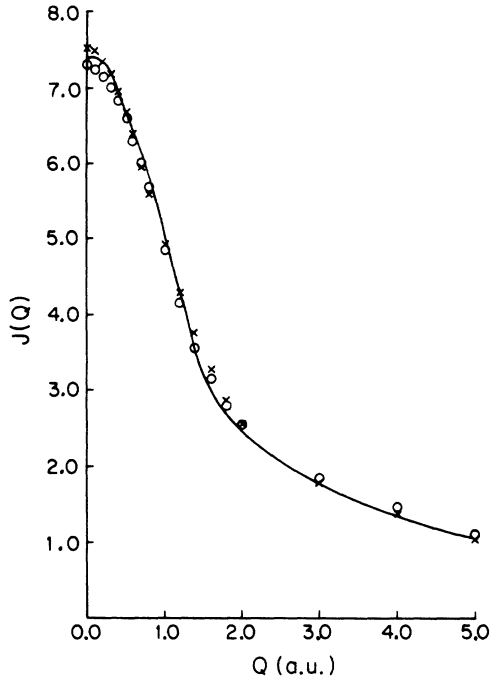

FIG. 7. Total Compton profile of niobium. ○ represents experimental points and × represents the results due to the RFA model. The solid curve is from the present calculations.

VII. MAGNETIC MOMENT

As mentioned previously, we employed the BNDPKG programs to search for a possible ferromagnetic state of bcc niobium and to determine the magnetic moment at large values of the lattice constant. A self-consistency convergence criterion of $10^{-4}\mu_B$ for the magnetic moment was employed in the calculations. Table VI gives the magnetic moment of Nb for several values of the lattice parameter. These results are also displayed in Fig. 8. The magnetic moment is zero for lattice constants up to 7.84 a.u. The self-consistent calculations converged to a state of nonzero magneton number at $a=7.85$ a.u. The transition to a magnetic state occurs after a 26% increase in the lattice constant beyond the equilibrium value. Moroever, Fig. 8 shows that as the *lattice constant* continues to increase, the magnetic moment also increases,

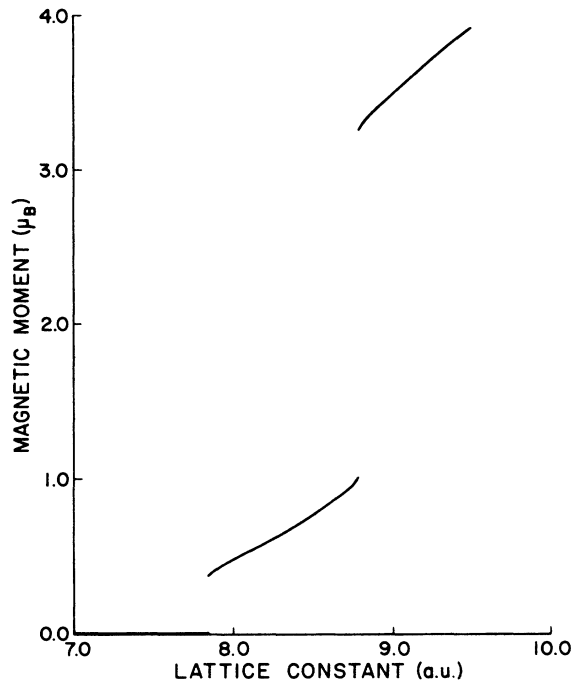

FIG. 8. Magnetic moment of bcc niobium vs lattice constant.

but with a discontinuous jump at about $a=8.80$ a.u. (a low-spin to high-spin transition).

Recently, Moruzzi *et al.*[70] have calculated a similar magnetic transitions in bcc vanadium by utilizing a fast augmented-spherical-wave, fixed-spin-moment procedure. They describe the transition as "type III." Our calculations show that the magnetic transition in Nb is also of type III. It must be pointed out, however, that we have not considered here the possibility of any other kind of magnetic order other than uniform ferromagnetism. Consequently, a final determination of the form of magnetic order expected in bcc Nb at large lattice constants will require further investigation.

VIII. CONCLUSION

The electronic band structure and density of states of Nb have been calculated in the present work using the LCGO method. A large enhancement of the density of states at the Fermi energy, presumably due to electron-phonon interactions, is indicated. The calculated Fermi surface shows a reasonable quantitative agreement with the de Haas–van Alphen data. The major structural features observed in the optical conductivity and Compton-profile observations are reproduced in the present investigation. The x-ray form factor compares well with the experimental findings. The total Compton profile is found to be in excellent agreement with the experimental measurements, while the calculation has not yielded a satisfactory amplitude in anisotropies. Body-centered-cubic niobium undergoes a type-III magnetic transition as the lattice constant is expanded. Transitions from a nonmagnetic to a low-spin state and from a low-spin state to a high-spin state are predicted. Finally, and in general, we believe that present study has produced satisfactory results for the electronic structure of niobium, indicating the utility of the LCGO method and density-functional theory.

TABLE VI. Lattice constant a and magnetic moment m for bcc Nb.

a (a.u.)	m (μ_B)
6.23–7.84	0.0
7.85	0.372
7.88	0.414
8.00	0.493
8.50	0.765
8.75	0.969
8.78	1.019
8.79	1.041
8.80	3.251
8.81	3.284
8.82	3.304
8.88	3.376
9.00	3.514
9.50	3.938

ACKNOWLEDGMENTS

One of us (A.R.J.) is thankful to the Council for International Exchange of Scholars, Washington, D.C., for financial support. This work was also supported in part by the U.S. National Science Foundation under Grant No. DMR-85-04259.

*Permanent address: Department of Physics, Sardar Patel University, Vallabh Vidyanagar 388120, Gujarat State, India.

[1]L. F. Mattheiss, Phys. Rev. B **1**, 373 (1970).
[2]J. R. Anderson, D. A. Papaconstantopoulos, J. W. McCaffrey, and J. E. Schirber, Phys. Rev. B **7**, 5115 (1973).
[3]G. S. Painter, J. S. Faulkner, and G. M. Stocks, Phys. Rev. B **9**, 2448 (1974).
[4]W. E. Pickett and P. B. Allen, Phys. Rev. B **11**, 3599 (1975).
[5]N. Elyashar and D. D. Koelling, Phys. Rev. B **13**, 5362 (1976).
[6]K. M. Ho, S. G. Louie, J. R. Chelikowsky, and M. L. Cohen, Phys. Rev. B **15**, 1755 (1977).
[7]N. Elyashar and D. D. Koelling, Phys. Rev. B **15**, 3620 (1977).
[8]L. L. Boyer, D. D. Papaconstantopoulos, and B. M. Klein, Phys. Rev. B **15**, 3685 (1977).
[9]J. F. Alward, C. Y. Fong, and C. G. Sridhar, Phys. Rev. B **18**, 5438 (1978).
[10]V. L. Moruzzi, J. F. Janak, and A. R. William, *Calculated Electronic Properties of Metals* (Pergamon, New York, 1978), p. 124.
[11]S. G. Louie, K. M. Ho, and M. L. Cohen, Phys. Rev. B **19**, 1774 (1979).
[12]C. L. Fu and K. M. Ho, Phys. Rev. B **28**, 5480 (1983).

[13]J. Neve, B. Sundqvist, and Ö. Rapp, Phys. Rev. B **28**, 629 (1983).
[14]V. P. Zhukov, V. A. Gubanov, and T. Jarlborg, J. Phys. Chem. Solids **46**, 1111 (1985).
[15]N. C. Bacalis, K. Blathras, P. Thomaides, and D. A. Papaconstantopoulos, Phys. Rev. B **32**, 4849 (1985).
[16]J. H. Kaiser, R. N. West, and N. Shiotani, J. Phys. F **16**, 1307 (1986).
[17]D. A. Papaconstantopoulos, in *Handbook of the Band Structure of Elemental Solids* (Plenum, New York, 1986), p. 137.
[18]N. I. Papanicolau, N. C. Bacalis, and D. A. Papaconstantopoulos, Z. Phys. B **65**, 453 (1987).
[19]R. A. Deegan and W. D. Twose, Phys. Rev. **164**, 997 (1967).
[20]S. Wakoh, Y. Kubo, and J. Yamashita, J. Phys. Soc. Jpn. **38**, 416 (1975).
[21]C. Y. Fong and M. L. Cohen, Phys. Lett. **44A**, 375 (1973).
[22]B. Chakraborty, W. E. Pickett, and P. B. Allen, Phys. Rev. B **14**, 3227 (1976).
[23]W. L. McMillan, Phys. Rev. **167**, 331 (1968).
[24]J. E. Kunzler and F. S. L. Hsu, Phys. Rev. B **1**, 366 (1970).
[25]G. B. Scott and M. Springford, Proc. R. Soc. London, Ser. A **320**, 115 (1970).
[26]J. R. Leibowitz, G. V. Blessing, and E. M. Alexander, Phys. Rev. B **9**, 2457 (1974).
[27]E. Fawcett, W. A. Reed, and R. Soden, Phys. Rev. **159**, 553 (1967).
[28]E. Fawcett, W. A. Reed, and R. R. Soden, Phys. Rev. **173**, 677 (1968).
[29]M. H. Halloran, J. H. Condon, J. E. Graebner, J. E. Kunzier, and F. S. L. Hsu, Phys. Rev. B **1**, 366 (1970).
[30]A. C. Thorson and T. G. Berlincourt, Phys. Rev. Lett. **7**, 244 (1961).
[31]G. B. Scott, M. Springford, and J. R. Stockton, Phys. Lett. **27A**, 655 (1968).
[32]D. P. Karim, J. B. Ketterson, and G. W. Crabtree, J. Low. Temp. Phys. **30**, 389 (1978).
[33]B. M. Powell, P. Martel, and A. D. B. Woods, Phys. Rev. **171**, 727 (1968).
[34]N. E. Alekseevskii, K. H. Bertel, and V. I. Nizhankovskii, Zh. Eksp. Teor. Fiz. Pisma Red. **19**, 117 (1974) [JETP Lett. **19**,72 (1974)].
[35]D. E. Eastman, Solid State Commun. **7**, 1697 (1969).
[36]I. Lindau and W. E. Spicer, Phys. Rev. B **10**, 2262 (1974).
[37]N. Shiotani, T. Okada, T. Mizoguchi, and H. Sekizwa, J. Phys. Soc. Jpn. **38**, 423 (1975).
[38]S. Wakoh, T. Fukamachi, S. Hosoya, and J. Yamashita, J. Phys. Soc. Jpn. **38**, 1601 (1975).
[39]N. G. Alexandropoulos and W. A. Reed, Phys. Rev. B **15**, 1790 (1977).
[40]M. Tomak, H. Singh, B. K. Sharma, and S. Manninen, Phys. Status Solidi B **127**, 221 (1985).
[41]J. M. Weaver, D. W. Lynch, and C. G. Olson, Phys. Rev. B **7**, 4311 (1973).
[42]A. I. Golovashkin, I. E. Leksina, G. P. Motulevich, and A. A. Shubin, Zh. Eksp. Teor. Fiz. **56**, 51 (1969) [Sov. Phys.—JETP **29**, 27 (1969)].
[43]E. S. Black, D. W. Lynch, and C. G. Olson, Phys. Rev. B **16**, 2337 (1977).
[44]M. M. Kirillova and L. V. Nomerovannaya, Fiz. Tverd. Tela (Leningrad) **20**, 984 (1978) [Sov. Phys.—Solid State **20**, 568 (1978)].
[45]V. V. Trung, L. J. LeBlanc, and G. J. Turpin, J. Opt. Soc. Am. **68**, 1017 (1978).
[46]A. I. Golovashkin and A. L. Shelekhov, Fiz. Tverd. Tela (Leningrad) **24**, 3339 (1982) [Sov. Phys.—Solid State **24**, 1897 (1982)].
[47]J. E. Holiday, in *Proceedings of the International Meeting of Electronic Structure of Metals and Alloys Studied by Methods of Band Structure Spectroscopy, Methods, Strathcylde, 1973*, edited by D. J. Fabin (Academic, New York, 1973), p. 251.
[48]V. V. Nemoshkalenko, V. P. Krivitskii, A. P. Nesenyuk, L. I. Nikolaev, and A. P. Shpak, J. Phys. Chem. Solids **36**, 277 (1975).
[49]R. Caillat, R. Fontaine, L. Feve, and M. J. Guittet, C. R. Hebd. Seances Acad. Sci. C **280**, 189 (1975).
[50]A. R. Shulman, V. V. Korablev, and Yu. A. Morozov, Izv. Akad. Nauk USSR **35**, 218 (1971) [Bull. Acad. Sci. USSR **35**, 199 (1971)].
[51]T. Kushida and J. C. Murphy, Phys. Rev. B **3**, 1574 (1971).
[52]W. R. Cox, D. J. Hayes, and F. R. Brotzen, Phys. Rev. B **7**, 3580 (1973).
[53]N. Morton, B. W. James, G. H. Wastenholm, and R. J. Nichols, J. Phys. F **5**, 85 (1975).
[54]G. A. Prinz, Phys. Rev. Lett. **54**, 1051 (1985).
[55]B. Heinrich, A. S. Arrot, J. F. Cochran, C. Liu, and K. Myrtle, J. Vac. Sci. Technol. A **4** 1376 (1986).
[56]J. G. Wright, Philos. Mag. **24**, 217 (1971).
[57]U. Gradmann, W. Kummerle, and P. Tillmans, Thin Solid Films **34**, 249 (1976).
[58]W. Keune, R. Malbauer, U. Gonser, J. Lauer, and D. L. Williamson, J. Appl. Phys. **48**, 2976 (1977).
[59]R. F. Willis, J. A. C. Bland, and W. Schwarzacher, J. Appl. Phys. **63**, 4051 (1988).
[60]C. Carbone, G. S. Sohal, E. Kisker, and E. F. Wassermann, J. Appl. Phys. **63**, 3499 (1988).
[61]J. Madsen and O. K. Anderson, in *Magnetism and Magnetic Materials—1975 (Philadelphia)*, Proceedings of the 21st Annual Conference on Magnetism and Magnetic Materials, edited by J. J. Becker, G. H. Lauder, and J. J. Rhyne (AIP, New York, 1978), p. 327.
[62]U. K. Poulsen, J. Kollar, and O. K. Anderson, J. Phys. F **6**, L241 (1976).
[63]O. K. Anderson, J. Madsen, U. K. Poulson, O. Jepsen, and J. Kollar, Physica **86-88B**, 249 (1977).
[64]J. Kubler, Phys. Lett. **81A**, 81 (1981).
[65]D. Bagayoko and J. Callaway, Phys. Rev. B **28**, 5419 (1983).
[66]J. Callaway, Xianwu Zou, and D. Bagayoko, Phys. Rev. B **27**, 631 (1983).
[67]D. Bagayoko, A. Zielger, and J. Callaway, Phys. Rev. B **27**, 7046 (1983).
[68]V. L. Moruzzi, P. M. Marcus, K. Schwarz, and P. Mohn, Phys. Rev. B **34**, 1784 (1986).
[69]J. L. Fry, X. Z. Zhao, N. E. Brener, G. Fuster, and J. Callaway, Phys. Rev. B **36**, 868 (1987).
[70]V. L. Moruzzi, P. M. Marucs, and P. C. Pattnaik, Phys. Rev. B **37**, 8003 (1988).
[71]C. S. Wang and J. Callaway, Comput. Phys. Commun. **14**, 327 (1978).
[72]J. Callaway and C. S. Wang, Phys. Rev. B **16**, 2095 (1977).
[73]C. S. Wang and J. Callaway, Phys. Rev. B **15**, 298 (1977).
[74]D. G. Laurent, C. S. Wang, and J. Callaway, Phys. Rev. B **17**, 455 (1978).
[75]P. Blaha and J. Callaway, Phys. Rev. B **12**, 7664 (1985).
[76]R. Poirier, R. Kari, and I. G. Csizmadia, *Physical Science Data, Vol. 34: Handbook of the Gaussian Basis Set* (Elsevier, New York, 1985), p. 632.
[77]O. Jepsen and O. K. Anderson, Solid State Commun. **9**, 1763 (1971).

[78]G. Lehman and M. Taut, Phys. Status Solidi B **54**, 469 (1972).
[79]J. Rath and A. J. Freeman, Phys. Rev. B **11**, 2109 (1975).
[80]S. P. Singhal, Phys. Rev. B **12**, 6007 (1975).
[81]S. P. Singhal, Phys. Rev. B **12**, 564 (1975).
[82]J. Rath, C. S. Wang, R. A. Tawil, and J. Callaway, Phys. Rev. B **8**, 5139 (1973).
[83]C. S. Wang and J. Callaway, Phys. Rev. B **11**, 2417 (1975).
[84]D. G. Laurent, J. Callaway, and C. S. Wang, Phys. Rev. B **20**, 1134 (1979).
[85]D. G. Laurent, J. Callaway, J. L. Fry, and N. E. Brener, Phys. Rev. B **23**, 4977 (1981).
[86]D. G. Laurent and J. Callaway, Phys. Lett. **84A**, 499 (1981).
[87]J. E. Holliday, in *The Electron Microprobe,* edited by T. D. McKinley, K. F. J. Meinrich, and D. B. Wittry (Wiley, New York, 1966), p. 10.
[88]V. V. Nemoshkalenko and V. P. Krivitskii, Ukr. Fiz. Zh. **13**, 1274 (1968) [Ukr. Phys. J. **13**, 911 (1969)].
[89]F. Heininger, E. Bucher, and J. Muller, Phys. Kondens. Mater. **5**, 243 (1966).
[90]Y. Nakagava and A. D. B. Woods, Phys. Rev. Lett. **11**, 271 (1963).
[91]Y. Nakagava and A. D. B. Woods, in *Lattice Dynamics,* edited by R. F. Wallis (Pergamon, Oxford, 1963), p. 39.
[92]W. Y. Ching and J. Callaway, Phys. Rev. B **11**, 1324 (1975).
[93]A. P. Lenham and D. M. Treherne, in *Optical Properties and Electronic Structure of Metals and Alloys,* edited by F. Abeles (North-Holland, Amsterdam, 1966) p. 196.
[94]J. F. Janak, A. R. Williams, and V. L. Moruzzi, Phys. Rev. B **11**, 1522 (1975).
[95]W. Y. Ching and J. Callaway, Phys. Rev. Lett. **30**, 441 (1973).
[96]W. Y. Ching and J. Callaway, Phys. Rev. B **9**, 5115 (1974).
[97]O. Terasaki, Y. Uchida, and D. Watanabe, J. Phys. Soc. Jpn. **39**, 1277 (1975).
[98]H. P. Hanson, F. Herman, J. D. Lea, and S. Skillman, Acta Crystallogr. **17**, 1040 (1964).
[99]F. Biggs, L. B. Mendelsohn, and J. B. Mann, At. Data Nucl. Data Tables **16**, 201 (1975).